Progressive RPE atrophy and photoreceptor death in *KIZ*-associated autosomal recessive retinitis pigmentosa

Yuchen Lin[a,b], **Christine L. Xu**[a,c], **Mark P. Breazzano**[c,d], **Akemi J. Tanaka**[e], **Joseph Ryu**[a,c], **Sarah R. Levi**[a,c], **Ke Yao**[b], **Janet R. Sparrow**[a,c,e], **Stephen H. Tsang**[a,c,e]

[a]Jonas Children's Vision Care and Bernard & Shirlee Brown Glaucoma Laboratory, Edward S. Harkness Eye Institute, New York-Presbyterian Hospital, New York, New York, USA

[b]Eye Center, Second Affiliated Hospital, School of Medicine, Zhejiang University, Hangzhou, Zhejiang, P. R. China

[c]Department of Ophthalmology, New York-Presbyterian Hospital, New York, New York, USA

[d]Department of Ophthalmology, New York University School of Medicine, New York, New York, USA

[e]Department of Pathology & Cell Biology, Institute of Human Nutrition, and Columbia Stem Cell Initiative, Columbia University, New York, New York, USA

Abstract

Background: To evaluate the long-term progression of autosomal recessive retinitis pigmentosa (RP) due to mutations in *KIZ* using multimodal imaging and a quantitative analytical approach.

Methods: Whole exome sequencing (WES) and targeted capture sequencing were used to identify mutation. Fundus photography, short-wavelength autofluorescence (SW-AF), spectral-domain optical coherence tomography (SD-OCT) imaging, and electroretinography (ERG) were analyzed. Serial measurements of peripheral retinal pigment epithelium (RPE) atrophy area with SW-AF, as well as the ellipsoid zone (EZ) width using SD-OCT were performed.

Results: Two homozygous variants in KIZ—a c.226C>T mutation as well as a previously unreported c.119_122delAACT mutation—were identified in four unrelated patients. Fundus examination and ERG revealed classic rod-cone dysfunction, and SD-OCT demonstrated outer retinal atrophy with centrally preserved EZ line. SW-AF imaging revealed hyperautofluorescent rings with surrounding parafoveal, mid-peripheral and widespread loss of autofluorescence. The RPE atrophy area increased annually by 4.9%. Mean annual exponential rates of decline for *KIZ* patients were 8.5% for visual acuity and 15.9% for 30 Hz Flicker amplitude. The average annual reduction distance of the EZ distance was 66.5 μm per year.

CONTACT Stephen H. Tsang sht2@cumc.columbia.edu Jonas Children's Vision Care and Bernard & Shirlee Brown Glaucoma Laboratory, Edward S. Harkness Eye Institute, New York-Presbyterian Hospital, New York, NY.

Conclusions: RPE atrophy progresses along with a loss of photoreceptors, and parafoveal RPE hypoautofluorescence is commonly seen in *KIZ*-associated RP patients. *KIZ*-associated RP is an early-onset severe rod-cone dystrophy.

Keywords

Introduction

Retinitis pigmentosa (RP) is a heterogeneous category of retinal dystrophies that is characterized by the degeneration of rods followed by gradual cone death. This condition is typically attributed to mutations affecting photoreceptors or retinal pigment epithelial (RPE) cells (1,2). The most common inheritance pattern for RP is autosomal recessive (50–60% of all RP), followed by autosomal dominant (30–40%), and X-linked (5–15%) (1).

Kizuna Centrosomal Protein (KIZ; OMIM#615757) is a centrosomal substrate of Polo-like kinase-1 (PLK1) that functions by regulating mitotic chromosome stability (3). Mutations in the *KIZ* gene have been recently reported to cause autosomal recessive RP (arRP) in seven individuals from five unrelated families (4–6). Patients with *KIZ*-associated RP exhibit fundus features of typical RP, such as waxy pale optic disc, retinal vascular attenuation, and bone spicule pigmentary changes along the arcades (4,5). However, how this ciliopathy affects different cell types in the retina is unknown.

In this study, we present the clinical characteristics, genetic findings, and long-term progression of four patients with RP caused by mutations in *KIZ*.

Patients and methods

Approval from the Institutional Review Board (IRB) ethics committee at Columbia University was obtained before undertaking this research project (IRB#AAAB6560). Ophthalmic examination notes were retrospectively reviewed in patients. Best-corrected visual acuity (BCVA), slit-lamp biomicroscopy, fundus examination, spectral-domain optical coherence tomography (SD-OCT) scans through the fovea, and short-wavelength fundus autofluorescence (SW-AF, 488 nm), were obtained in all four affected patients with Spectralis HRA+OCT (Heidelberg Engineering, Heidelberg, Germany). Full-field electroretinogram (ERG) testing was performed according to the International Society for Clinical Electrophysiology of Vision (ISCEV) standards (7).

Genetic testing was performed in all four patients in this study, using either whole exome sequencing (WES, A-II:2, B-II:1, and D-II:5) or targeted capture sequencing of 280 retinal dystrophy-related genes (C-II:1).

The horizontal length of the intact ellipsoid zone (EZ) line in SD-OCT and the hypoautofluorescent areas representative of RPE atrophy in SW-AF were measured using ImageJ (Bethesda, MD, USA).

Snellen BCVA was converted to logMAR units for comparison. LogMAR units were used to quantify low vision, where hand motion = 2.0 (8). All analyses were performed using SPSS Statistics for Windows, version 23 (IBM, Armonk, NY, USA).

Results

This study includes four unrelated, *KIZ*-associated RP patients (A-II:2, B-II:1, C-II:1, and D-II:5) with a mean age of 48 ± 18.9 years (Figure 1). The homozygous variant c.226C>T was identified in individuals A-II:2, C-II:1, and D-II:5 (Figure 1). Individual B-II:1 is the first reported patient to harbor a pathogenic homozygous disruptive variant c.119_122delAACT. A summary of the affected individual genotypes is listed in Table 1.

The patients in this study exhibited chorioretinal phenotypes characteristic of RP (Figure 1). All patients initially presented with night blindness followed by progressive constriction of their visual field. Notably, three of the four patients (A-II:2, B-II:1, C-II:1) retained normal visual acuity from the first visit. However, the visual acuity of patient D-II:5 deteriorated to hand motion in both eyes by age 49 (Table 2), which suggests rapid photoreceptor death. The mean annual exponential rate of decline for visual acuity in the *KIZ* patients in this study was 8.5%.

In SD-OCT scans, the length of the EZ line (distance between the temporal to nasal terminations of the band) was found to decrease in three patients (A-II:2, B-II:1, and D-II:5) with disease progression (Figure 2a, Supplemental Tables 1–3). The average annual reduction distance was 66.5 μm per year. In SW-AF images, the area of RPE atrophy was found to increase with disease progression (Figure 2b), with a mean annual increase of 4.9%.

ERG recordings were collected from three patients (A-II:2, B-II:1, and D-II:5) (Figure 3). For A-II:2 at 60 years of age and D-II:5 at age 37 years of age, ERG rod responses of the right eyes were almost undetectable. The mean 30-Hz response amplitude at the first visit (18.6 μV) was reduced by 80.8% from the age-matched mean normal of 96.8 μV. The mean cone 30-Hz flicker implicit time (35.3 milliseconds) was significantly delayed from the age-matched mean normal of 29.3 milliseconds. At their most recent visits, all patients except B-II:1 (rod amplitude, 39.6 μV, OD; 43.3 μV, OS; data not shown) had undetectable rod responses. A longitudinal study of individuals A-II:2 and D-II:5 revealed that the amplitudes of the 30-Hz Flicker exhibited a downward trend, the mean annual rates of decline was 15.9%. These findings point to a severe, early-onset rod-cone dystrophy.

Discussion

The KIZ protein localizes to the outer nuclear layer of the retina, specifically the bottom of the cilia and basal body of cilium-associated centrioles (4). To date, over 30 genes have been reported to be associated with ciliopathy (RetNet: https://sph.uth.edu/retnet/), which can lead to either non-syndromic or syndromic retinal degeneration. Here, we described the clinical characteristics and disease progression of *KIZ*-associated RP.

The presence of EZ has been reported to be associated with better visual acuity in RP patients, and the absence of EZ may reflect a foveal dysfunction (9). In this study, the mean annual exponential rate of decline for visual acuity in the patients with *KIZ* mutation in this study was 8.5%. In particular, the visual acuity of patient D-II:5 significantly decreased during the past eight years, which can be attributed to macular dystrophy, indicated by the short remaining EZ line. It is worth noting that the visual acuity of the left eye of patient B-II:1 was significantly reduced, but the EZ line length did not shorten faster than his right eye. Patient B-II:1 had no other eye diseases beside RP. It is not clear whether this is related to the deletion of important domains of the KIZ by the mutation of deletion (c.119_122delAACT) in patient B-II:1 rather than the missense mutation (c.226C>T) in the other three patients. Long-term observation and further study of KIZ are needed to elucidate causative mechanisms.

The mean EZ line reduction distance was 66.5 μm per year among all the patients with *KIZ* mutations in this study. Although the decreased rate was smaller than that of the previously reported RP patients, the EZ line distance at the first visits was shorter than those found in published studies (10–12). This indicates that photoreceptor atrophy had developed long before the visual field loss among the patients in this study.

According to longitudinal data, all the patients with a *KIZ* mutation showed a significant increase in the dark adaptation threshold, which suggests that night vision loss occurred before the first visit. ERG rod response amplitudes were severely attenuated or extinguished. The mean annual rate of decline in cone 30-Hz flicker response among patients with *KIZ* mutations was 15.9%, which is higher than the average annual decline rate of 10% per year that was reported among RP patients (13–16).

SW-AF images showed that area of RPE atrophy increased 4.9% annually among the patients with *KIZ* mutations in this study. A previous study using wide-field FAF showed that the extent of abnormal FAF is related to the visual field in patients with chorioretinitis; and it was also suggested that, as in patients with RP, the location and size of the scotoma correspond spatially to the area of abnormal FAF (17). We suspect that the RPE atrophy area expansion rate can objectively reflect the visual function, and provide an estimate of RP disease progression. Notably, individual C-II:1 exhibited preserved central autofluorescence surrounded by a hyperautofluorescent ring of variable diameter at 21 years old, while the other three patients (A:II-2, B:II-1 and D:II-5), in later stages of the disease, have significantly more severe RPE atrophy concentrated in the peripheral region of the hyperautofluorecent ring, indicating severe rod damage.

Consistent with these findings, *KIZ* is associated with severe phenotypes. Comparing with other ciliopathy-associated arRP genes such as *C2orf71*, *MAK* and *FAM161A*, which are characterized by milder RP phenotypes without macular involvement or steep progression like *KIZ* (18–22). It is not clear why different ciliopathies have variable phenotypes; longer courses of observation and further studies are necessary to elucidate this finding.

In summary, we observed progressive, arRP without syndromic features in patients with missense or deletion mutations in *KIZ*. RPE atrophy appears to gradually increase along

with a progressive loss of photoreceptors. Additionally, *KIZ*-associated RP patients are commonly associated with parafoveal RPE hypoautofluorescence, as compared to non-syndromic RP patients. *KIZ*-associated RP is a severe early-onset rod-cone dystrophy.

Supplementary Material

Refer to Web version on PubMed Central for supplementary material.

Acknowledgments

References

1. Hartong DT, Berson EL, Dryja TP. Retinitis pigmentosa. Lancet.2006;368:1795–809. doi:10.1016/S0140-6736(06)69740-7. [PubMed: 17113430]

2. Hamel C. Retinitis pigmentosa. Orphanet J Rare Dis. 2006;1:40. doi:10.1186/1750-1172-1-40. [PubMed: 17032466]

3. Oshimori N, Ohsugi M, Yamamoto T. The Plk1 target Kizunastabilizes mitotic centrosomes to ensure spindle bipolarity. Nat Cell Biol. 2006;8:1095–101. doi:10.1038/ncb1474. [PubMed: 16980960]

4. El Shamieh S, Neuille M, Terray A, Orhan E, Condroyer C,Demontant V, Michiels C, Antonio A, Boyard F, Lancelot ME, et al. Whole-exome sequencing identifies KIZ as a ciliary gene associated with autosomal-recessive rod-cone dystrophy. Am J Hum Genet. 2014;94:625–33. [PubMed: 24680887]

5. Gustafson K, Duncan JL, Biswas P, Soto-Hermida A, Matsui H,Jakubosky D, Suk J, Telenti A, Frazer KA, Ayyagari R. Whole genome sequencing revealed mutations in two independent genes as the underlying cause of retinal degeneration in an Ashkenazi Jewish Pedigree. Genes (Basel). 2017;8:210. doi:10.3390/genes8090210.

6. El Shamieh S, Mejecase C, Bertelli M, Terray A, Michiels C,Condroyer C, Fouquet S, Sadoun M, Clerin E, Liu B, et al. Further insights into the ciliary gene and protein KIZ and its murine ortholog PLK1S1 mutated in rod-cone dystrophy. Genes (Basel). 2017;8:277.

7. McCulloch DL, Marmor MF, Brigell MG, Hamilton R, Holder GE, Tzekov R, Bach M. ISCEV standard for full-field clinical electroretinography (2015 update). Doc Ophthalmol. 2015;130:1–12. doi:10.1007/s10633-014-9473-7.

8. Tibbetts MD, Shah CP, Young LH, Duker JS, Maguire JI, Morley MG. Treatment of acute retinal necrosis. Ophthalmology. 2010;117:818–24. doi:10.1016/j.ophtha.2009.09.001. [PubMed: 20079537]

9. Aizawa S, Mitamura Y, Baba T, Hagiwara A, Ogata K, Yamamoto S. Correlation between visual function and photoreceptor inner/outer segment junction in patients with retinitis pigmentosa. Eye (Lond). 2009;23:304–08. doi:10.1038/sj.eye.6703076. [PubMed: 18188175]

10. Sujirakul T, Lin MK, Duong J, Wei Y, Lopez-Pintado S, Tsang SH.Multimodal imaging of central retinal disease progression in a 2-year mean follow-up of retinitis pigmentosa. Am J Ophthalmol. 2015;160:786–798 e784. doi:10.1016/j.ajo.2015.06.032.

11. Cabral T, Sengillo JD, Duong JK, Justus S, Boudreault K, Schuerch K, Belfort R Jr., Mahajan VB, Sparrow JR, Tsang SH Retrospective analysis of structural disease progression

in retinitis pigmentosa utilizing multimodal imaging. Sci Rep. 2017;7:10347. doi:10.1038/s41598-017-10473-0.

12. Takahashi VKL, Xu CL, Takiuti JT, Apatoff MBL, Duong JK,Mahajan VB, Tsang SH. Comparison of structural progression between ciliopathy and non-ciliopathy associated with autosomal recessive retinitis pigmentosa. Orphanet J Rare Dis. 2019;14:187. doi:10.1186/s13023-019-1163-9. [PubMed: 31370859]

13. Birch DG, Anderson JL, Fish GE. Yearly rates of rod and cone functional loss in retinitis pigmentosa and cone-rod dystrophy. Ophthalmology. 1999;106:258–68. doi:10.1016/S0161-6420(99)90064-7. [PubMed: 9951474]

14. Berson EL. Long-term visual prognoses in patients with retinitispigmentosa: the Ludwig von Sallmann lecture. Exp Eye Res. 2007;85:7–14. doi:10.1016/j.exer.2007.03.001. [PubMed: 17531222]

15. Berson EL, Rosner B, Weigel-DiFranco C, Dryja TP, Sandberg MA. Disease progression in patients with dominant retinitis pigmentosa and rhodopsin mutations. Invest Ophthalmol Vis Sci. 2002;43:3027–36. [PubMed: 12202526]

16. Mendes HF, van der Spuy J, Chapple JP, Cheetham ME. Mechanisms of cell death in rhodopsin retinitis pigmentosa: implications for therapy. Trends Mol Med. 2005;11:177–85. doi:10.1016/j.molmed.2005.02.007. [PubMed: 15823756]

17. Seidensticker F, Neubauer AS, Wasfy T, Stumpf C, Thurau SR,Kampik A, Kernt M. Wide-field fundus autofluorescence corresponds to visual fields in chorioretinitis patients. Clin Ophthalmol. 2011;5:1667–71. doi:10.2147/OPTH.S26224. [PubMed: 22174575]

18. Gerth-Kahlert C, Tiwari A, Hanson JVM, Batmanabane V, Traboulsi E, Pennesi ME, Al-Qahtani AA, Lam BL, Heckenlively J, Zweifel SA, et al. C2orf71 mutations as a frequent cause of autosomal-recessive retinitis pigmentosa: clinical analysis and presentation of 8 novel mutations. Invest Ophthalmol Vis Sci. 2017;58:3840–50. [PubMed: 28763557]

19. Collin RW, Safieh C, Littink KW, Shalev SA, Garzozi HJ, Rizel L,Abbasi AH, Cremers FP, den Hollander AI, Klevering BJ, et al. Mutations in C2ORF71 cause autosomal-recessive retinitis pigmentosa. Am J Hum Genet. 2010;86:783–88. [PubMed: 20398884]

20. van Huet RA, Siemiatkowska AM, Ozgul RK, Yucel D, Hoyng CB, Banin E, Blumenfeld A, Rotenstreich Y, Riemslag FC, den Hollander AI, et al. Retinitis pigmentosa caused by mutations in the ciliary MAK gene is relatively mild and is not associated with apparent extra-ocular features. Acta Ophthalmol. 2015;93:83–94. [PubMed: 25385675]

21. Di Gioia SA, Letteboer SJ, Kostic C, Bandah-Rozenfeld D, Hetterschijt L, Sharon D, Arsenijevic Y, Roepman R, Rivolta C. FAM161A, associated with retinitis pigmentosa, is a component of the cilia-basal body complex and interacts with proteins involved in ciliopathies. Hum Mol Genet. 2012;21:5174–84. doi:10.1093/hmg/dds368. [PubMed: 22940612]

22. Van Schil K, Klevering BJ, Leroy BP, Pott JW, Bandah-Rozenfeld D,Zonneveld-Vrieling MN, Sharon D, den Hollander AI, Cremers FP, De Baere E, et al. A nonsense mutation in FAM161A is a recurrent founder allele in Dutch and Belgian individuals with autosomal recessive retinitis pigmentosa. Invest Ophthalmol Vis Sci. 2015;56:7418–26. [PubMed: 26574802]
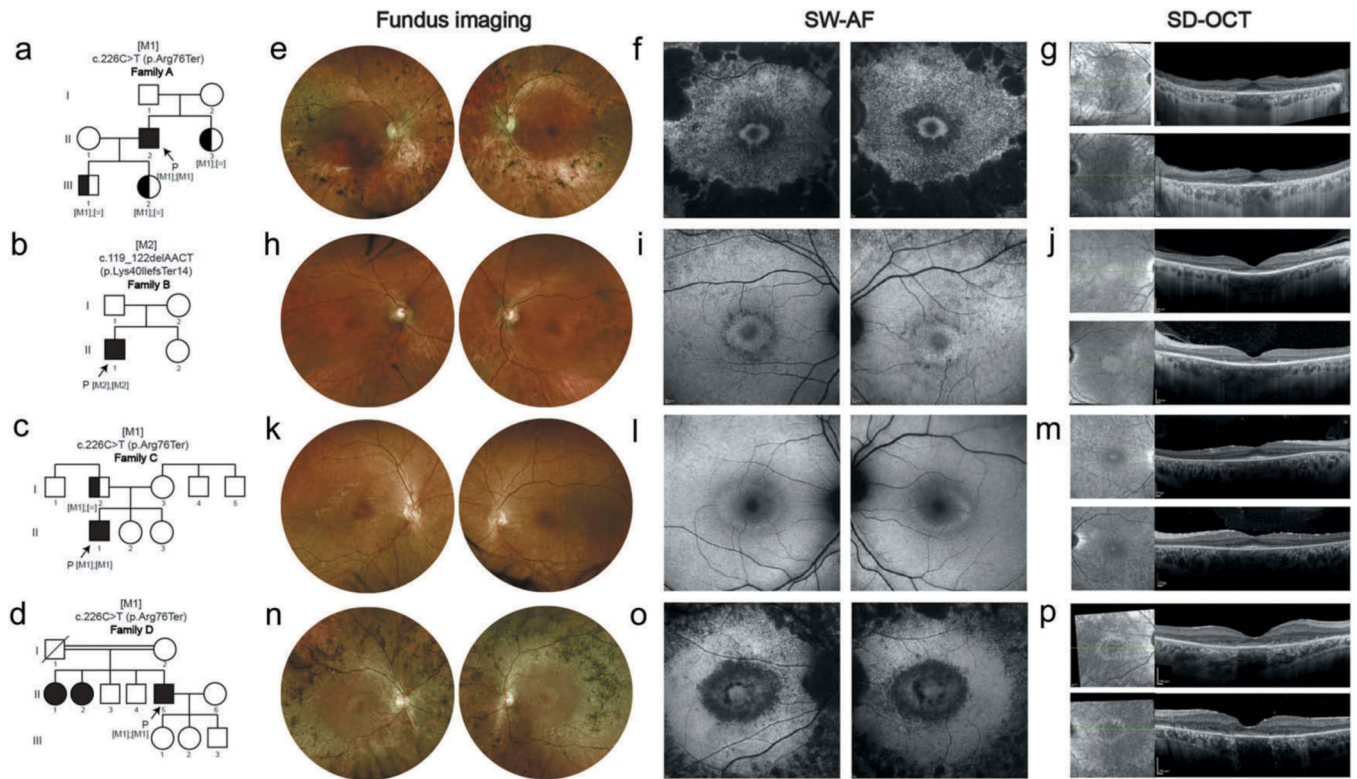
Figure 1.

Early parafoveal RPE loss in four individuals affected with RP.

(a-d) Pedigrees of family A-D are demonstrated. Equal signs denote the wild-type allele, square boxes indicate males, circles indicate females, and affected individuals are pointed out in black. Arrows indicate the probands. Double-line indicates consanguineous marriages. M1, and M2 depict the positions of the mutations identified in this study. (e-g) Images of both eyes of A-II:2 at 62-year-old. Fundus imaging (e) shows attenuated vessels, waxy pallor of the optic disc, atrophic changes and bone spicule pigmentation in the midperiphery area. SW-AF (f) reveals a hyperautofluorescent ring surrounding the central area of the macula with surrounding parafoveal and mid-peripheral severe flaky or fused hypoautofluorescence. SD-OCT (g) reveals outer retinal atrophy with centrally preserved RPE and ellipsoid zone (EZ) line, with hypertransmission outside the corresponding area of choroid. (h-j) Images of both eyes of B-II-1 at 60-year-old. Fundus imaging (h), SW-AF (i), and SD-OCT (j) show moderate pigmentary changes in peripheral retina outside the vascular arcades with hyperautofluorescent ring around the macular, and surrounding parafoveal and mid-peripheral mottling hypoautofluorescence, as well as outer retinal atrophy with centrally preserved RPE and EZ line, with hypertransmission outside the corresponding area of choroid. (k-m) Images of both eyes of C-II:1 at 21-year-old. Fundus imaging (k), SW-AF (l), and SD-OCT (m) show mild pigmentary changes in peripheral retina outside the vascular arcades, and hyperautofluorescent ring around the macula with mild parafoveal loss of autofluorescence, as well as thinning of the outer retina with centrally preserved RPE and EZ line. (n-p) Images of both eyes of D-II:5 at 49-year-old. Fundus imaging (n) shows severe pigmentary changes with bone spicule pigmentation, as well as attenuated vessels,

and the waxy pallor of the optic disc. Hyperautofluorescent ring surrounding the normal-looking macular and surrounding parafoveal and mid-peripheral severe flaky and mottling hypoautofluorescence are seen on SW-AF (o). SD-OCT images (p) reveal outer retinal atrophy with centrally preserved RPE and ellipsoid zone (EZ) line, with hypertransmission outside the corresponding area of choroid.
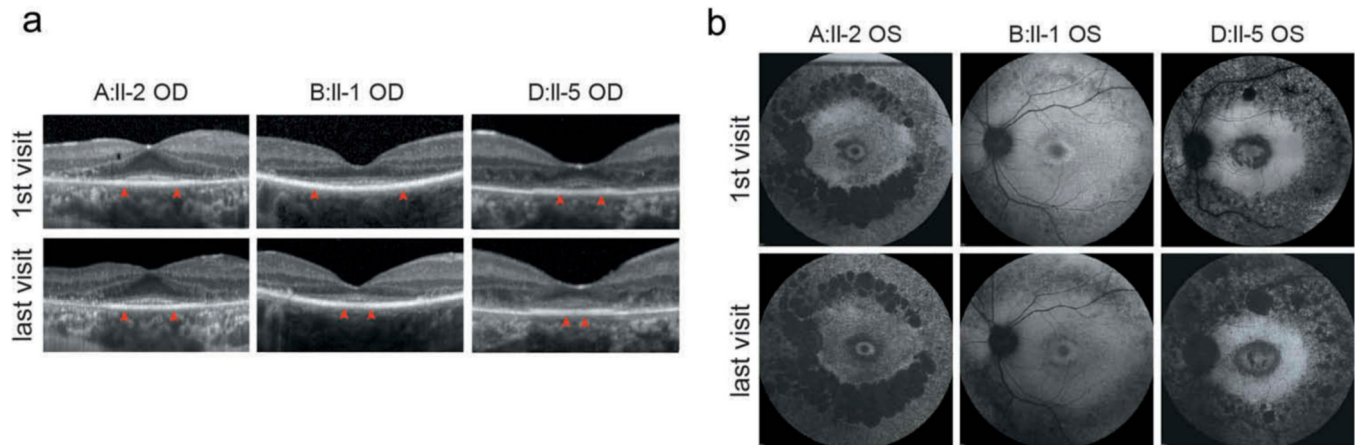
Figure 2.
Progressive Ellipsoid zone loss. (a) SD-OCT imaging in patients A-II:2, B-II:1 and D-II:5 of the first visit and last visit (right eye) what was interval between visits. Red arrows show the boundaries of intact EZ lines. (b) SW-AF imaging in patients A-II:2, B-II:1 and D-II:5 of the first visit and last visits (left eye), accompanied by significant fusion and punctate enlargement of the hypoautofluorescence area in the parafoveal, mid-peripheral, and widespread retina within the disease course.
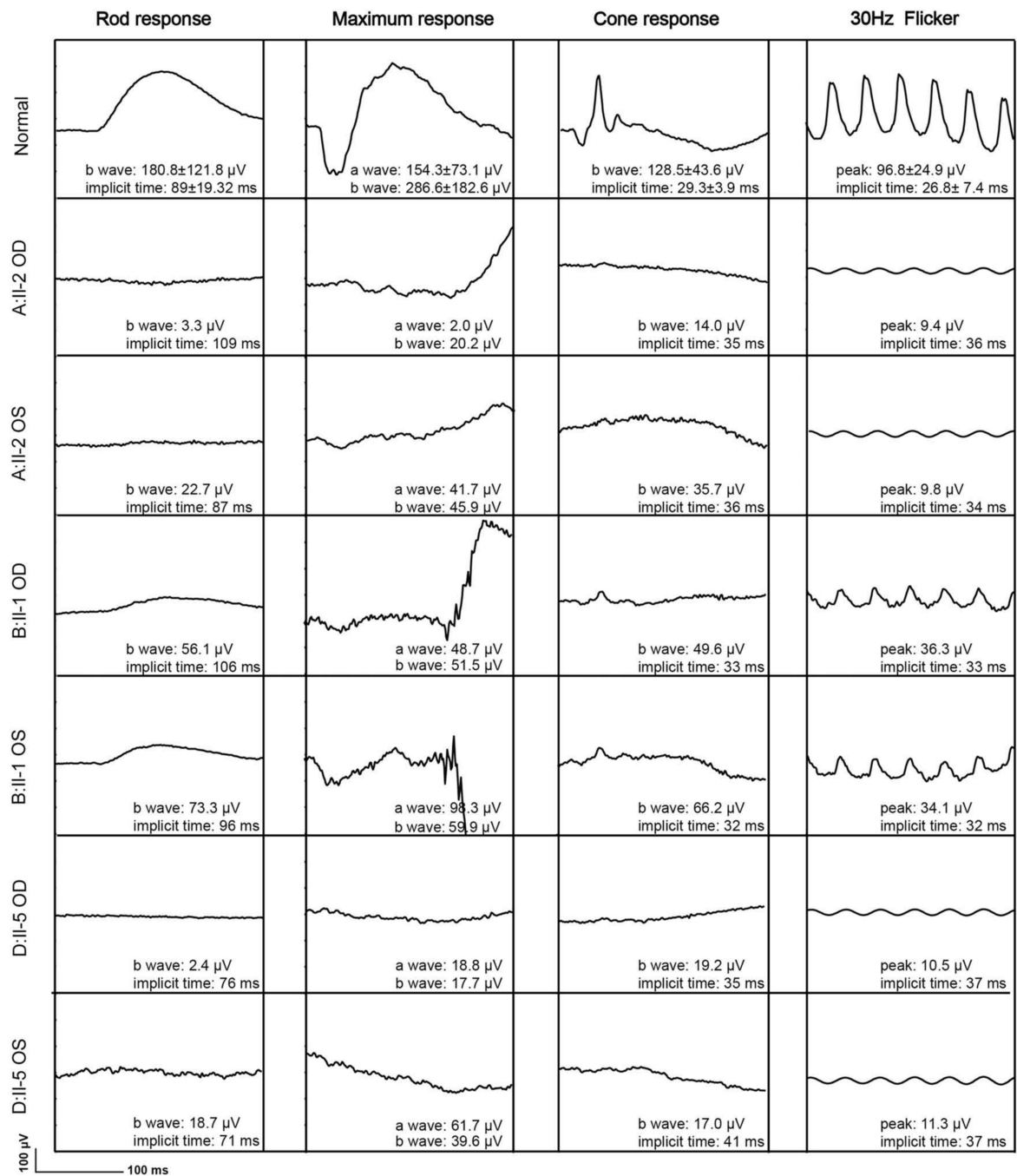
Figure 3.

Relative cone-functional 30-Hz preservation. Full-field electroretinography (ffERG) in patients A-II-2 (62-year-old), B-II:1 (60-year-old), and D-II:5 (49-year-old) with *KIZ*-related retinitis pigmentosa. FfERG demonstrated that scotopic rod-specific responses and photopic singe-flash responses were extinguished in patients A-II:2 and D-II:5, with diminished amplitudes in patient B-II:1. Maximal ERG and photopic 30-Hz amplitudes were reduced in all the three patients.

Table 1.

Summary of affected individual genotypes.

ID	*KIZ variant*	Protein consequence	Frequency of variant in control (gnomAD) database	Prediction
A-II:2	c.226C>T	p.Arg76Ter	0.0004433	Pathogenic
B-II:1	c.119_122delAACT	p.Lys40llefsTer14	0.00003832	Pathogenic
C-II:1	c.226C>T	p.Arg76Ter	0.0004433	Pathogenic
D-II:5	c.226C>T	p.Arg76Ter	0.0004433	Pathogenic

Table 2.

Summary of ocular phenotype and demographics in patients studied.

ID	Age of onset, sex	Age at 1st visit	Age at last visit	VA 1st RE/LE	VA last RE/LE
A-II:2	41, M	57	62	20/40, 20/50	20/30, 20/40
B-II:1	50, M	57	60	20/30, 20/80	20/60, 20/400
C-II:1	20, M	21	21	20/30, 20/25	NA, NA
D-II:5	35, M	35	49	20/150, 20/150	HM, HM

Ages are indicated in years.

Abbreviations are as follows: VA = visual acuity; LE = left eye; RE = right eye; HM = hand motion; NA = not available; M = male.